Available online at www.sciencedirect.com
SCIENCE DIRECT®
Vision Research 44 (2004) 209–220
Vision Research
www.elsevier.com/locate/visres

Time-varying, slow-phase component interaction in congenital nystagmus ☆

J. Shallo-Hoffmann [a,*], L.F. Dell'Osso [b,c,d], S. Dun [b,d]

[a] College of Optometry, Nova Southeastern University, 3200 South University Drive, Ft. Lauderdale, FL 33328, USA
[b] The Ocular Motor Neurophysiology Laboratory, Veterans Affairs Medical Center, Case Western Reserve University and University Hospitals of Cleveland, Cleveland, OH, USA
[c] Department of Neurology, Case Western Reserve University and University Hospitals of Cleveland, Cleveland, OH, USA
[d] Department of Biomedical Engineering, Case Western Reserve University and University Hospitals of Cleveland, Cleveland, OH, USA

Received 10 July 2002; received in revised form 6 August 2003

Abstract

We investigated the nystagmus of a 12-year-old boy with suspected X-linked congenital nystagmus (CN) and exophoria to determine the underlying mechanisms and component signals in the 'dual-velocity' and other slow phases of his Asymmetric (a)Periodic Alternating Nystagmus (APAN). Fast Fourier transforms (FFT) were performed on the waveforms and residual data after subtracting a sawtooth waveform whose amplitude and frequency matched those of the jerk nystagmus. The FFT analyses identified two frequency components (jerk—4 Hz and pendular—4 and 8 Hz, variable) that varied differently in intensity and frequency/phase over the time-course of the APAN. We synthesized each of the patient's slow phases using summation of sawtooth and sinusoidal waveforms. The resulting waveforms included jerk (with different slow-phase appearances), dual jerk, and pendular. We demonstrated that the pendular nystagmus seen during the neutral phase of APAN and the appearance of either decelerating (mimicking latent nystagmus), dual-velocity, or dual-jerk slow phases can be explained and produced by the summation of linear and pendular components of variable amplitudes and frequencies/phases. Thus, one mechanism may be responsible for all the variation seen in this patient's slow phases, rather than the less parsimonious hypothesis of a switched-tonic-imbalance mechanism that we had originally suggested to simulate the dual-velocity waveform.

Keywords: Congenital nystagmus; Asymmetric aperiodic alternating nystagmus; Pendular and jerk waveforms; Mechanism; Fourier

1. Introduction

In some individuals with congenital nystagmus (CN), the nystagmus appears to be cyclical. It grows and falls in one direction (active phase), followed by a transition phase, and then grows and falls in the other direction, followed by another transition phase. However, unlike the acquired form of periodic alternating nystagmus (PAN), the two active phases in CN are often (but not always) unequal in length and the total period can vary in length from cycle to cycle. The term "Asymmetric (a)Periodic Alternating Nystagmus (APAN)" is used to differentiate the congenital form, which is thought to stem from an asymmetric, usually aperiodic oscillation of the neutral position, from the acquired form (Daroff & Dell'Osso, 1974). APAN is prevalent (approximately 30% of the cases) in patients with albinism (Abadi & Pascal, 1994) and CN without sensory deficits (Shallo-Hoffmann, Faldon, & Tusa, 1999). Although APAN is a complex version of periodic alternating nystagmus, it can be recognized clinically and can be described accurately with eye movement recordings. Its cause is unknown but may be related to a failure in calibration of the vestibular system (Leigh, Robinson, & Zee, 1981). In the unidirectional jerk waveforms of CN, the slow-phase waveforms may be exponentially accelerating, linear, or a combination of the two. The slow phases take the eye away from the target and saccades in the opposite direction return the eye to the target (foveating saccades).

☆ This work was supported in part by the Office of Research and Development, Medical Research Service, Department of Veterans Affairs.
* Corresponding author. Tel.: +1-954-262-4226; fax: +1-954-262-3875/1818.
E-mail address: shoffman@nova.edu (J. Shallo-Hoffmann).

0042-6989/$ - see front matter © 2003 Elsevier Ltd. All rights reserved.
doi:10.1016/j.visres.2003.09.007

The purpose of this study is to investigate the waveform characteristics of a patient with a nystagmus that exhibits a linear (constant velocity) slow-phase as the nystagmus grows during the active phase and an underlying, ever-present pendular nystagmus that becomes more prominent as the nystagmus falls off until the waveform is purely pendular during the transition phase (Dell'Osso, Shallo-Hoffmann, & Moore, 2000; Dun, Shallo-Hoffmann, & Dell'Osso, 2001). One peculiar waveform contained two segments of constant velocity. Since a tonic imbalance produces a linear slow phase, this *dual-velocity* waveform initially suggested a hypothetical control consisting of two different tonic imbalances and a switching mechanism (Dell'Osso et al., 2000). Since the nystagmus is unusual, it may shed light on basic elements that interact to develop APAN and CN waveforms.

2. Methods

2.1. Recording and protocol

The patient sat in a dimly lit room and was instructed to fixate a stationary LED (4 mm in diameter) located in the primary position, at a distance of 155 cm. Head movements were minimized using a chin and head rests. Eye movements were recorded for an average of 4–5 min. Binocular horizontal eye movements were recorded using an infrared limbal reflection technique (frequency response, 100 Hz; resolution, 0.1°; range ±20°) Skalar (Delft, The Netherlands). Eye movements were calibrated monocularly and binocularly before and after the recording session. The eye position signals were digitized at 250 Hz and stored on computer for off-line analysis.

2.2. Analysis

Data analysis (and filtering, if required), statistical computation of means and standard deviations, and graphical presentation were performed using custom software written in MATLAB (The MathWorks, Natick MA). Each nystagmus cycle begins at the start of the slow phase that defoveates the target and ends after the fast phase that refoveates the target (or, if present, after the period of extended foveation). Similarly, the length of an interval of either the jerk left (JL) or jerk right (JR) nystagmus is measured from the beginning of the first of many consecutive slow phases to the end of the last corresponding consecutive fast phase. Thus, the length of a transition phase is from the end of the preceding interval of jerk nystagmus to the beginning of the next interval of jerk nystagmus (i.e., from the end of the last consecutive fast-phase cycle to the beginning of the first consecutive slow-phase cycle). This provides a consistent method of determining the lengths of the various phases of APAN despite variations in the waveforms. The length, or period, of a PAN or APAN cycle is the sum of the JL phase, transition phase between jerk left and jerk right (N_{L-R}), jerk right (JR) phase, and transition phase between jerk right and jerk left (N_{R-L}). Compared to the phases of acquired PAN, which are well known to be regular and symmetric (e.g., JL: 90 s; N_{L-R}: 15 s; JR: 90 s; N_{R-L}: 15 s; Period = 210 s), recordings of CN subjects have shown that the APAN of CN is asymmetric and the cycle is usually much longer (e.g., JL: 90 to >1000 s; N_{L-R}: 0 to >20 s; JR: 90 to >1000 s; N_{R-L} : 0 to >20 s; Period = $\geqslant$ 180 to >2000 s). As Fig. 1 shows, transition phases may consist of either immediate direction changes, periods of little or no nystagmus, periods of alternating direction nystagmus, or periods of pendular nystagmus. The above definitions apply equally to each type and provide a consistent method to measure cycle lengths of both acquired PAN and the more complex congenital APAN.

Both fast Fourier transforms (FFT) and power spectral densities were performed on sections of representative data for each type of slow-phase waveform, carefully chosen to contain little or no variation. Hanning windows were used to prevent aliasing and our frequency resolution was 1.25 Hz. The frequency spectra allowed us to identify the peak frequencies of these constructed "stationary" waveforms, as has been done in the past for eye and head movements in CN (Dell'Osso, Van der Steen, Steinman, & Collewijn, 1992). Since the FFT's and power spectral densities yielded essentially the same results, only the former are presented. The FFT's were calculated for the specific waveforms shown and do not represent the spectra of the variable waveforms during the whole APAN cycle.

2.3. Computer simulation

The ocular motor system simulation was designed and implemented using the Simulink component of MATLAB, a control systems simulation package capable of performing simulations in both continuous and discrete time.

3. Case history

A 12 year-old boy with suspected x-chromosomal, recessively inherited CN and exophoria had APAN with mean cycle durations ranging from 140 to 185 s. Snellen VA: 20/60 (0.33), Near: J3 (N6). He had an intermittent, variable left head turn (~10°) and never exhibited a right head turn. Neurological and ophthalmological examinations, ERG, VEP, and MRI were normal. The study was performed according to the guidelines of the Declaration of Helsinki and was approved by the hospital's institutional review board. Both the patient and his

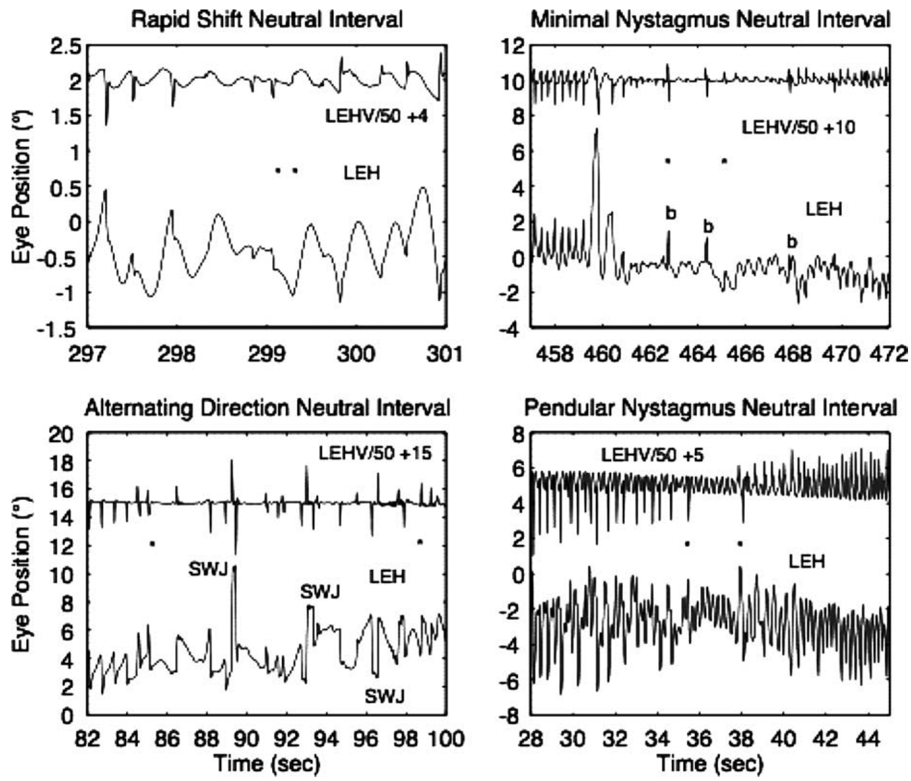

Fig. 1. Four panels illustrating different types of neutral intervals in congenital Asymmetric, (a)Periodic Alternating Nystagmus (APAN). Top left: a rapid shift (1 s) from a left-beating interval (jerk left) to a right-beating interval (jerk right). Top right: an interval (~3 s) with little nystagmus between the left-beating interval (pseudo jerk right) and the right-beating interval (pseudo jerk left). Bottom left: an interval (14 s) containing both left- and right-beating waveforms between the left-beating interval (jerk left) and the right-beating interval (jerk right). Bottom right: an interval (3 s) of pendular nystagmus between the left-beating interval (jerk left to dual jerk left) and the right-beating interval (jerk right to dual jerk right). LEH—left eye horizontal; LEHV—left eye horizontal velocity (shown scaled by 50 and shifted as indicated); SWJ—square-wave jerk; b—blink; *—beginnings and ends of neutral intervals, as determined from the waveforms (see text). In all figures, rightward is up and leftward is down.

parent were fully informed about the nature of the procedures and gave written consent before the beginning of testing. The child signed an assent form and one parent signed a consent form.

4. Results

Ocular motility recordings of this subject's APAN revealed variability in the timing of the intervals of jerk nystagmus, in the types of waveforms recorded, and in the individual slow phases of the specific waveforms themselves.

4.1. APAN cycle and neutral intervals

The transition phases separating jerk nystagmus in one direction from oppositely directed jerk nystagmus were usually characterized by intervals of pendular nystagmus. Fig. 2 shows a transition phase (also called, neutral interval) between the end of a jerk left nystagmus phase and the beginning of jerk right. Prior to the purely pendular interval, cycles of dual jerk left nystagmus are evident (Dell'Osso & Daroff, 1975), (that is, jerk left with a superimposed, higher frequency pendular nystagmus) between 21 and 28 s. The initial and final cycles of jerk intervals in both directions contained dual jerk cycles, suggesting that the pendular oscillation may be masked by high-frequency, high-slow-phase velocity beats of jerk nystagmus. Over each APAN cycle, the slow-phase velocity rose sharply in one direction and remained high for approximately 50% of the interval before slowly diminishing; after the nystagmus reversed direction, a similar variation of slow-phase velocity occurred in the opposite direction. The jerk left and jerk right phases were asymmetric with values of over 100 s in each direction. The two neutral intervals were also asymmetric, with the jerk-left-to-jerk-right interval (approximately 10 s) being longer than the jerk-right-to-jerk-left interval (a few seconds).

4.2. Waveforms exhibited

Throughout the intervals of jerk nystagmus in both directions there was variability in waveform and slow phases in addition to the expected amplitude variability.

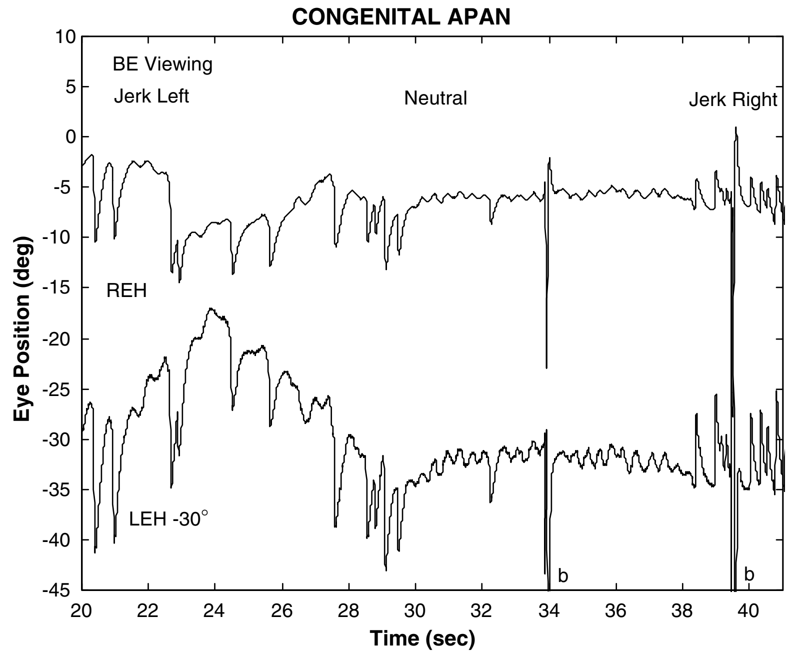

Fig. 2. Horizontal eye position vs. time plots for both eyes of this patient during the transition from a jerk-left interval through a neutral interval with a 3 Hz pendular nystagmus and into a jerk-right interval. BE—both eyes; REH—right eye horizontal; LEH—left eye horizontal (shown shifted left by 30° for clarity); b—large triphasic deflections indicating blinks.

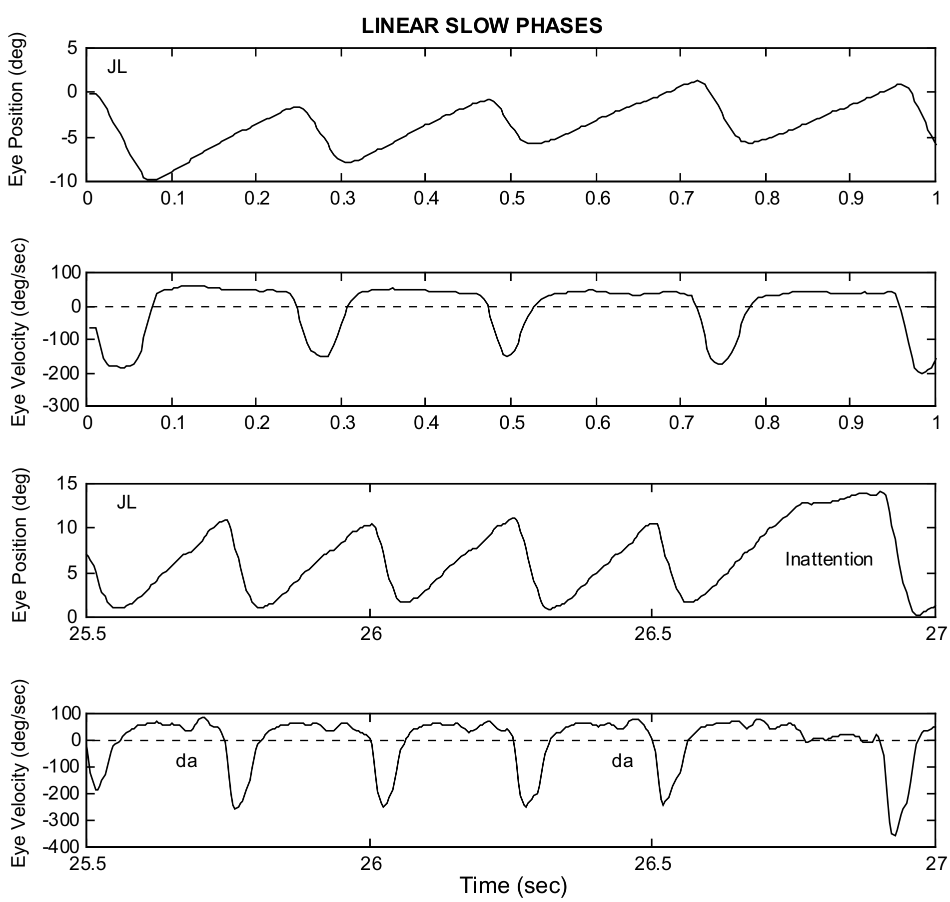

Fig. 3. Horizontal eye position and velocity during intervals of typical jerk-left nystagmus with linear slow phases, including one cycle demonstrating the effects of visual inattention (last cycle in bottom panels). da—instances of discrete accelerations. In this and the following figures, JL—jerk-left nystagmus.

The basic jerk waveform had linear slow phases. Fig. 3 (top two panels) shows an example of a jerk left interval with constant-velocity slow phases. The final cycle in the lower two panels is an example of an extended, low-velocity slow phase (approximately 0°/sec) produced by momentary *visual* inattention (i.e., a relaxation of 'fixation attempt') and interrupted by a belated fast phase. Such inattention can always be interrupted (and the nystagmus reinitiated) by reminding the subject to "look at the target."

Fig. 4 (upper two panels) illustrates discrete decelerations, commonly found in saccades (Abel, Traccis, Troost, & Dell'Osso, 1987; Schmidt, Dell'Osso, Abel, & Daroff, 1980) but also seen in some of the slow phases of this subject's jerk nystagmus (lower two panels). In both saccades and slow phases, discrete decelerations appear as abrupt decreases in slope in the position record or step decreases in the velocity record. Although caused by different mechanisms in the two instances, they each suggest a discrete change in the motor (control) signal driving the eyes.

As the upper panels of Fig. 5 show, these *dual-velocity* slow phases (that is, constant-velocity slow phases whose velocity (or slope) changes abruptly in midcourse) occurred in successive cycles at different times in the jerk intervals. The cycle at 36 s can also be considered a dual jerk cycle. In the lower panels of Fig. 5, a jerk right cycle is followed by a series of dual jerk right cycles, as indicated by the arrows. The effects of variable visual attention on the tail ends of the otherwise linear slow phases are evident in several of the cycles as a deceleration of the lengthened slow phases. These cycles resemble those of latent/manifest latent nystagmus (LMLN) but the CN fast phases are foveating, not defoveating.

In Fig. 6 (top two panels) an interval of dual jerk waveforms is shown in which the pendular component is seen to vary in amplitude and frequency on a cycle-to-cycle basis as the underlying slow-phase velocity is also varying. The net result is dual jerk right waveforms that become more sporadic and differ from each other in all characteristics; this was followed by a transition phase. In the two lower panels, a pendular nystagmus is seen superimposed on the accelerating slow phases of jerk right with extended foveation waveforms (JR_{ef}) producing unusual dual jerk right with extended foveation

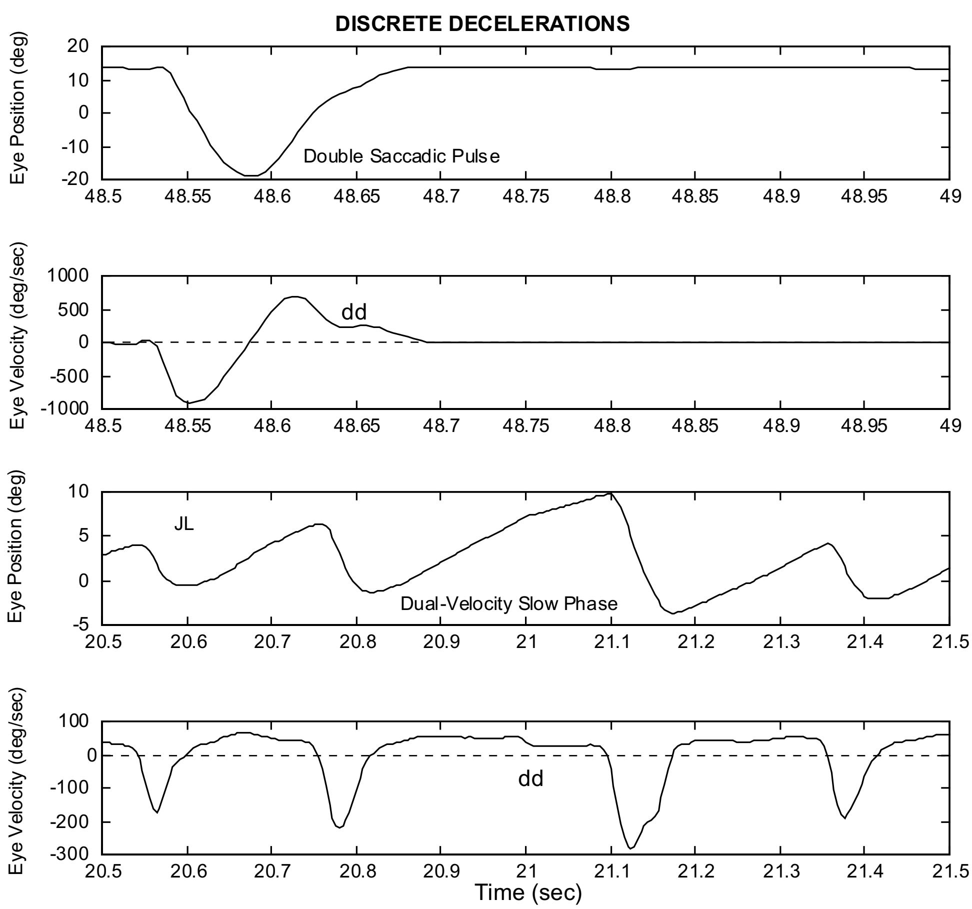

Fig. 4. Illustrations of discrete decelerations (not from this patient) in the horizontal position and velocity during a double saccadic pulse (top panels) and a slow-phase of JL nystagmus of this patient (bottom panels). In this and the following figures, dd—instances of discrete decelerations.

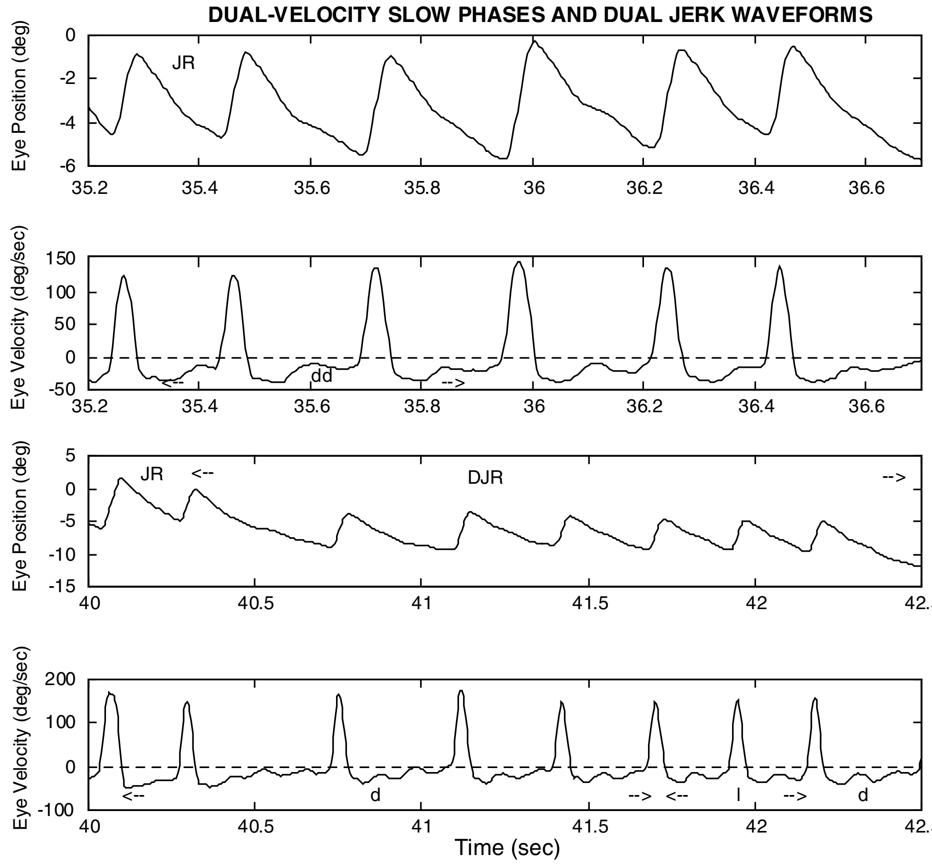

Fig. 5. Horizontal position and velocity records during dual-velocity slow phases of jerk-right nystagmus (top panels) and during dual jerk right (DJR) waveforms (bottom panels). In this and the following figures, JR—jerk right nystagmus; d—decelerating slow phases; l—linear slow phases. Arrowheads delimit intervals of indicated waveform or slow-phase type.

waveforms (DJR_{ef}). Some of the fast phases appear to have dynamic overshoots but they may reflect the pendular component.

Fig. 7 demonstrates both mixed slow phases of jerk right nystagmus (upper two panels) and mixed waveforms (lower two panels). In the first two cycles of the upper two panels, the slow phases accelerate and then decelerate; they are followed by a cycle of jerk nystagmus with a decelerating slow phase, five cycles with dual-velocity slow phases, another cycle with a decelerating slow phase, and finally two cycles with dual-velocity slow phases. This type of slow-phase variability was common and was due to variability in the pendular component. In the lower two panels mixtures of jerk right and jerk right with extended foveation waveforms are seen, also with variable slow phases as in the upper two panels.

4.3. Fast fourier transform waveform analysis

In an effort to better understand the underlying mechanisms that might produce the above variability, Fast Fourier transform (FFT) analyses were performed on the waveforms with dual-velocity slow phases, dual-jerk slow phases, and mixed slow phases respectively. Fig. 8A shows an interval of a dual-velocity, slow-phase waveform with its FFT; the dominant frequencies are 3.6 and 7.9 Hz. In Fig. 8B, an interval of dual jerk nystagmus is shown with its FFT; the dominant frequencies are 4.1 and 8.8–9.1 Hz. In Fig. 8C, an interval of mixed slow-phase waveforms is shown with its FFT; the dominant frequencies are 4.1 and 8.9–9.0 Hz. Note that these subtle changes in the amplitude (3.5°–7.2°) and frequency (3.6–4.1 Hz) of the pendular component result in the variable appearances of the slow phases.

4.4. FFT residual data analysis

To separate the pendular and jerk components, a sawtooth was fitted for each waveform and was subtracted from it. FFT were then performed on the residual data. Fig. 9A (top panel) shows the interval of a dual-velocity, slow-phase waveform with a fitted sawtooth and the residual of their difference. In this and Fig. 9B and C, the high-frequency portions coinciding with the fast phases are due to the imperfect subtraction during the fast phases (i.e., saccades have curvature due to acceleration and deceleration whereas the sawtooth

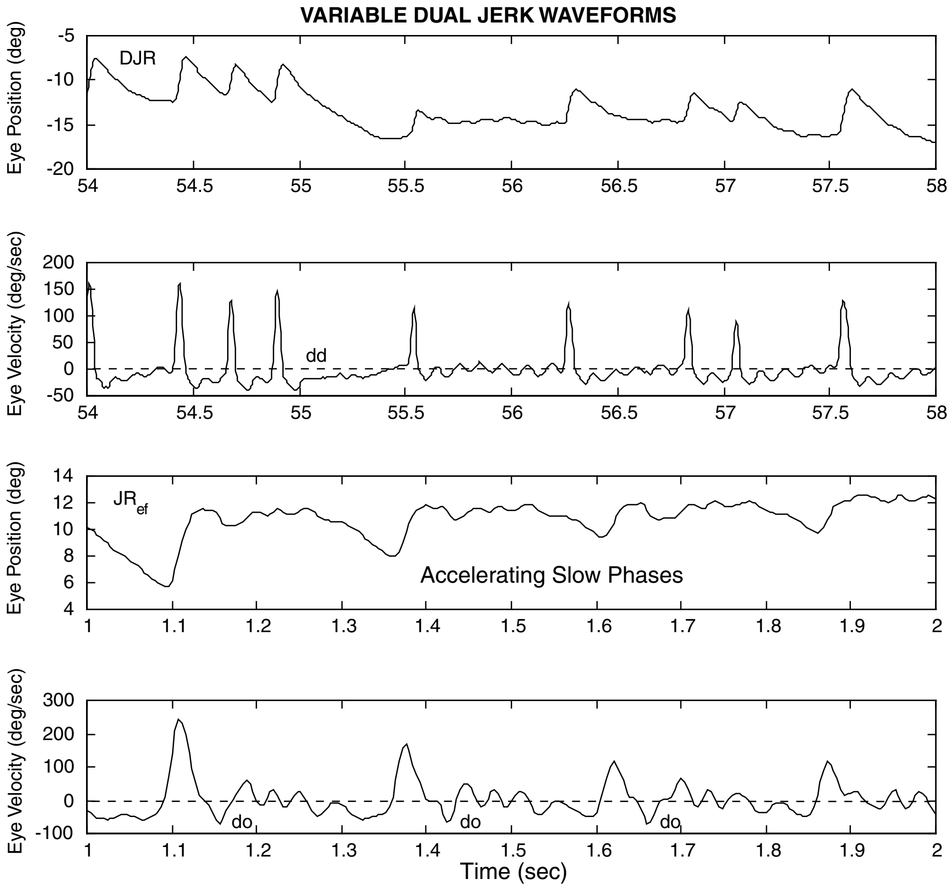

Fig. 6. Horizontal position and velocity records during variable dual jerk right nystagmus (top panels) and during jerk right with extended foveation (JR_{ef}) nystagmus waveforms showing the accelerating slow phases (bottom panels). do—dynamic overshoots.

was linear). The FFT of the residual is shown in the bottom panel; the dominant frequencies are 3.9 and 7.7–7.8 Hz. In Fig. 9B (top panel), the interval of dual jerk nystagmus with a fitted sawtooth and the residual of their difference is shown. The FFT of the residual is shown in the bottom panel; the dominant frequencies are 3.8–4.3 and 7.5–7.8 Hz. In Fig. 9C (top panel), the interval of mixed slow-phase waveform with a fitted sawtooth and the residual of their difference is shown. The FFT of the residual is shown in the bottom panel; the dominant frequencies are 4.1–4.4 and 7.7–8.1 Hz.

4.5. Waveform synthesis

In an attempt to recreate the pendular components of the waveforms, a sine wave was then fitted to the above residual data from each waveform. This was then combined with the fitted sawtooth to recreate each waveform. In Fig. 10A–C (top panels) the residuals and fitted sinusoids are shown for the dual velocity, dual jerk, and mixed slow-phase waveforms respectively. In the bottom panels of each, the components and their sums are shown for each waveform.

5. Discussion

We have analyzed the waveforms and inter-waveform transitions exhibited by an individual with CN and APAN with a rare combination of waveforms. The results of this analysis and waveform synthesis using components identified from the analysis, have provided insights into the specific mechanisms and subsystem instabilities that may underlie many of the waveforms common in CN.

5.1. Waveforms imply mechanisms

From the analysis of the slow-phase waveforms of CN, arise hypothetical mechanisms that may be responsible for the oscillations. Understanding these mechanisms is a first step in attempting to arrive at therapeutic interventions to damp the CN and improve potential visual acuity. Linear slow phases, present in LMLN, CN or vestibular nystagmus (VN) are produced by a tonic imbalance in either the vestibular, optokinetic, or push-pull neural integrator subsystems. Accelerating slow phases (pathognomonic in CN) are the result of an

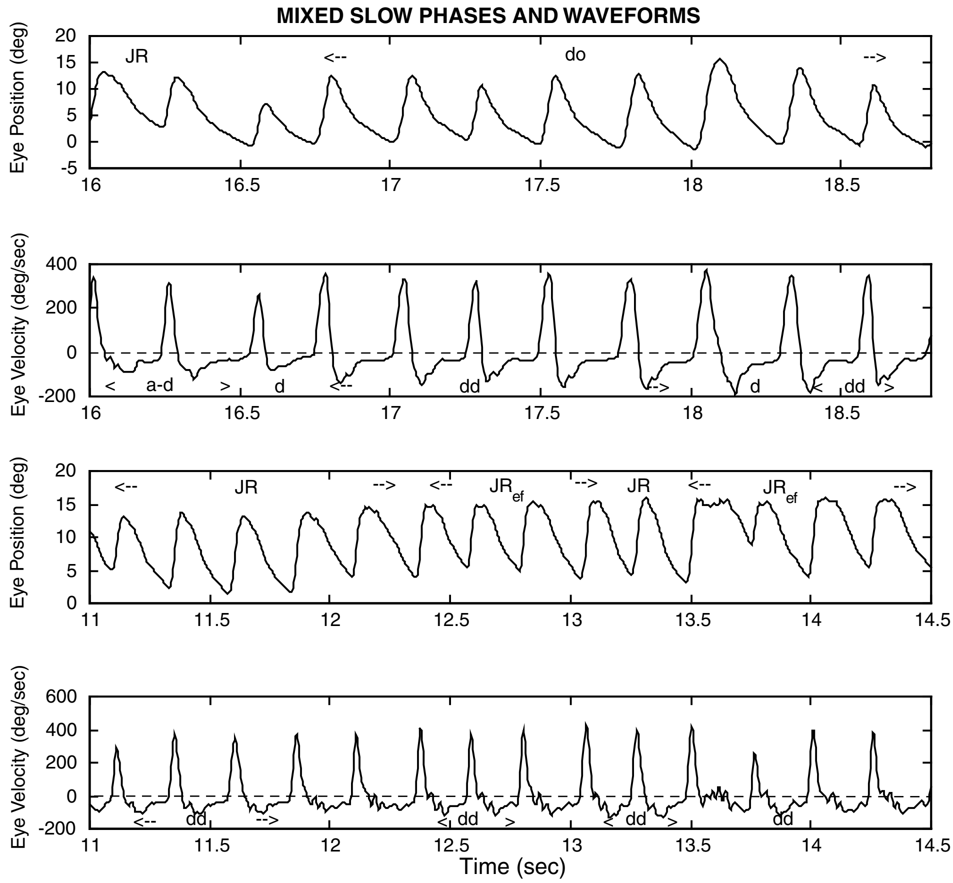

Fig. 7. Horizontal position and velocity records showing mixed slow phases during JR nystagmus (top panels) and during mixed nystagmus waveforms (bottom panels). a–d—accelerating then decelerating slow phase. Arrowheads delimit intervals of indicated waveform, or fast- or slow-phase type.

inherently unstable portion of the ocular motor system. Mathematically, they may be produced by a right-half-plane pole in a subsystem transfer function (e.g., neural integrator feedback loop). Decelerating slow phases (present in LMLN, saccadic pulses, and gaze-evoked nystagmus) are produced by a drift towards primary position (or another equilibrium point) as a result of an unintegrated saccadic pulse. Pendular slow phases (present in CN, LMLN, and acquired nystagmus) are the result of a portion of the ocular motor system having an oscillatory instability and are produced by a pair of $j\omega$-axis poles in a subsystem transfer function (e.g., in CN, the smooth-pursuit internal feedback loop).

5.2. FFT waveform and residual data analysis

The spectral analysis of the different waveforms identified two main frequency components (≅4 and ≅8–9 Hz) that varied differently in intensity and frequency over the time-course of the APAN. The 4-Hz component was the jerk frequency or the combination of jerk and pendular frequency. However, the 8-Hz component could be either the pendular frequency or the second harmonic of the jerk frequency and therefore, the individual components could not be separated.

The spectral analysis of the residual data also identified two main separate frequency components (≅4 Hz and ≅8 Hz). For the dual-velocity waveform, since the linear sawtooth was subtracted, the main peak, 3.9 Hz, was apparently the pendular frequency. And the secondary peak, 7.7–7.8 Hz, was a harmonic. Therefore, this dual-velocity slow-phase had an ≅4 Hz jerk component and an ≅4 Hz pendular component. Similarly, the mixed slow-phase waveform also had an ≅4 Hz jerk component and an ≅4 Hz pendular component. For the dual-jerk waveform, the main peak at ≅8 Hz was the pendular frequency. And the 3.8 Hz secondary peak was caused by the imperfect subtraction. Therefore, this dual-jerk waveform had an ≅4 Hz jerk component and an ≅8 Hz pendular component. Thus, each waveform had a ≅4 Hz jerk component with a linear slow-phase (presumably from the visuo-vestibular system) and either ≅4 Hz or ≅8 Hz pendular components that determined the ultimate shape of the slow phase. Pure jerk nystagmus with linear slow phases are not the most common waveforms in CN, although they are seen more

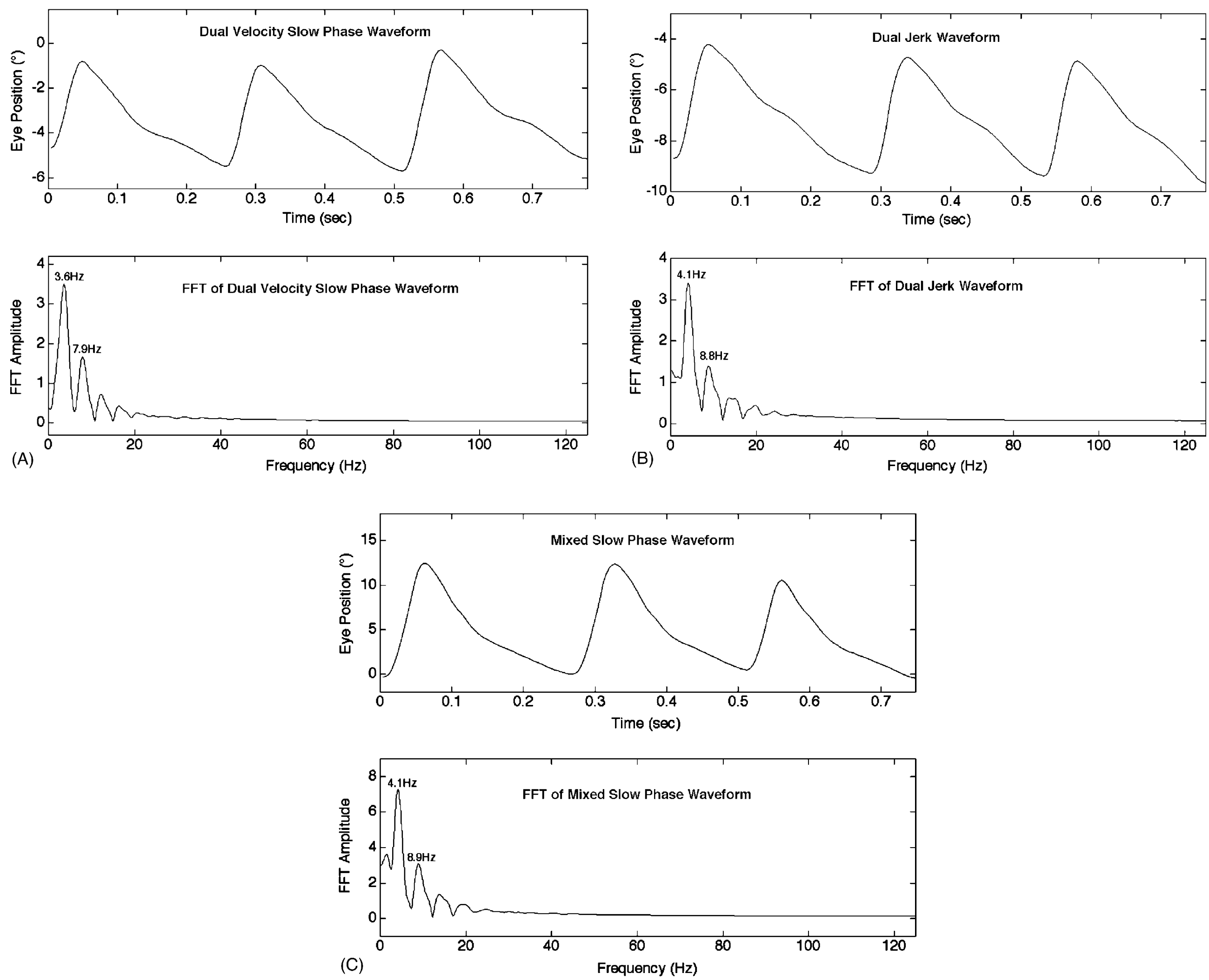

Fig. 8. (A) Top panel: Dual-velocity waveform. Bottom panel: Fast Fourier transform of the waveform in this figure only, presuming it was the result of a stationary process. In this and the following figures, FFT—fast Fourier transform. (B) Top panel: Dual jerk waveform. Bottom Panel: Fast Fourier transform of the waveform in this figure only, presuming it was the result of a stationary process. (C) Top panel: Mixed slow-phase waveform. Bottom panel: Fast Fourier transform of the waveform in this figure only, presuming it was the result of a stationary process.

in APAN. The ≅4 Hz pendular oscillation may stem from the same pursuit-system oscillation that is hypothesized to underlie pendular and pseudopendular CN waveforms (Dell'Osso & Jacobs, 2000; Jacobs, 2001; Jacobs & Dell'Osso, 2000) and the ≅8 Hz oscillation is common to dual-jerk waveforms seen in both CN and LMLN. The low-amplitude, high-frequency pendular oscillation of the dual jerk waveforms sometimes seen in LMLN may stem from oscillation in the circuitry of the nucleus of the optic tract (Hoffmann, 1983; Tusa, Mustari, Das, & Boothe, 2002).

5.3. Waveform synthesis and variability

By adding the fitted sine wave and the previously fitted sawtooth waveform, dual-velocity, dual-jerk, and mixed slow-phase waveforms were all synthesized, demonstrating that these complex time-variable waveforms may consist of two simple, albeit variable, components. As stated in Section 1, the unique occurrence of dual-velocity linear slow phases may have been due to either abrupt changes in tonic imbalance or in the Alexander's law variation of a constant tonic imbalance. Without an accurate recording system, they can easily be mistaken for decelerating slow phases. However, all three of the waveforms exhibited by this subject with CN and APAN could be synthesized by the addition of two commonly seen CN waveforms (jerk and pendular) with varying amplitudes and frequencies. The need to postulate a complex switching mechanism between two different steady-state tonic imbalances and the logic needed to control it has been alleviated by the more parsimonious explanation above. The variation in this patient's slow-phase waveforms over time and the

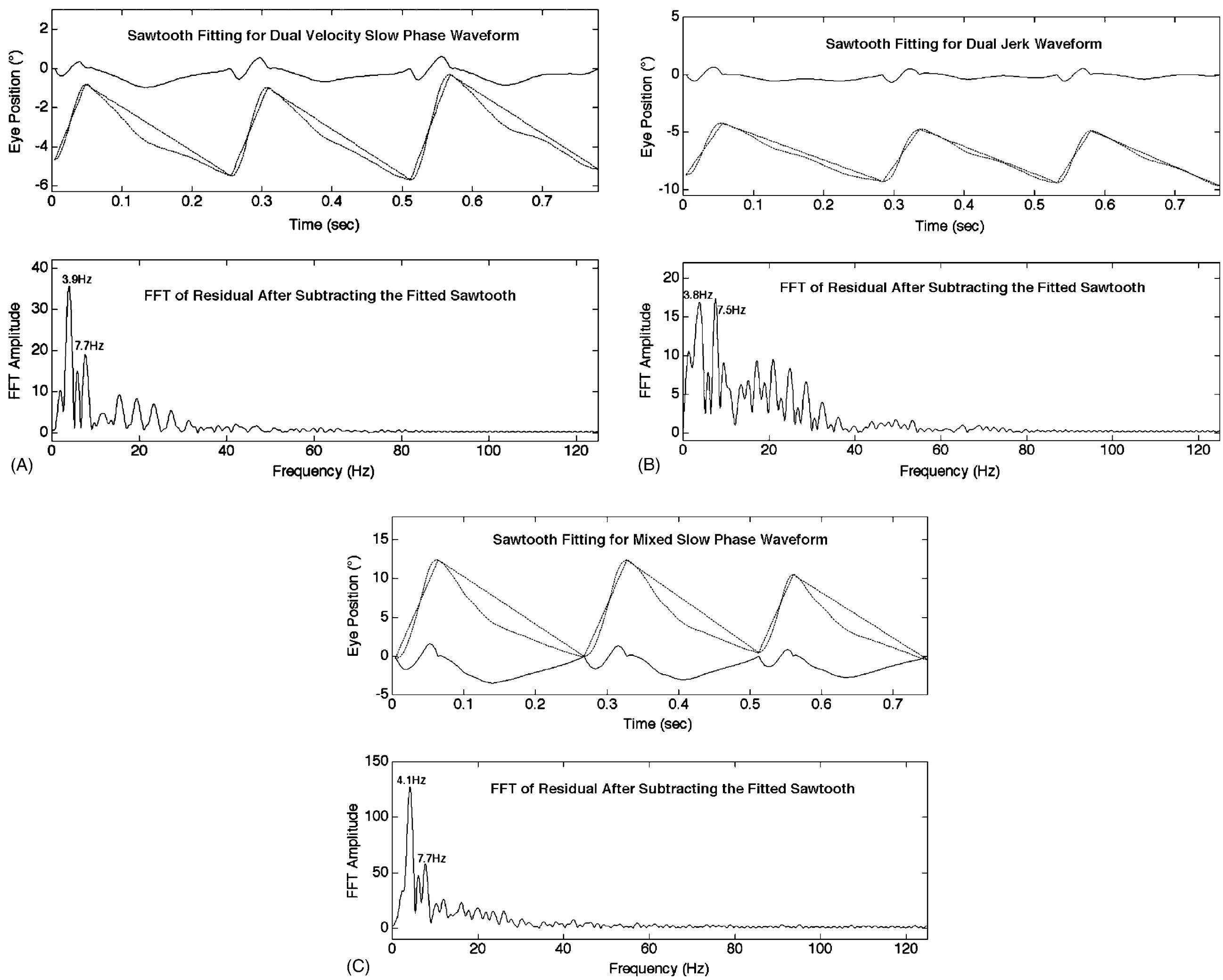

Fig. 9. (A) Top panel: Sawtooth fitting of a stationary dual-velocity waveform (both dashed) with the residual (solid). Bottom panel: Fast Fourier transform of the residual. (B) Top panel: Sawtooth fitting of a stationary dual jerk waveform (both dashed) with the residual (solid). Bottom panel: Fast Fourier transform of the residual. (C) Top panel: Sawtooth fitting of a stationary mixed slow-phase waveform (both dashed) with the residual (solid). Bottom panel: Fast Fourier transform of the residual.

spontaneous inter-beat variation suggest that several distinct instabilities are present to varying degrees. As one instability becomes dominant, its associated waveform is exhibited, only to be replaced by another type of instability, with its characteristic waveform. The above transitions from one waveform to another takes place during the time-varying changes in tonic imbalance secondary to the APAN. When more than one type of instability becomes dominant, mixed waveforms result. This is common in both CN and LMLN with their dual jerk waveforms. Variable-amplitude and -frequency/phase pendular oscillations superimposed on jerk nystagmus slow phases can also produce both accelerations and decelerations in the same slow phase. Such variable decelerations are to be distinguished from the repetitive decelerations seen in the slow phases of LMLN or gaze-evoked nystagmus.

5.4. Infantile nystagmus syndrome

The results of this study, lend evidence to a recent model of complex pendular CN waveforms (Dell'Osso & Jacobs, 2000; Jacobs, 2001; Jacobs & Dell'Osso, 2000) and suggest that the waveforms of CN may be caused by at least two separate instabilities: an undamped velocity oscillation in the pursuit system, underlying the pendular CN waveforms; and the linear jerk nystagmus from a vestibular imbalance, underlying the various jerk CN waveforms. In addition to waveforms specific to CN, is the low-amplitude, high-frequency pendular oscillation of dual jerk waveforms seen in both CN and LMLN. What has emerged from the past three decades of research into the waveforms of CN is the realization that "CN" is not a single type of nystagmus, as this oft-maligned name implies, but a syndrome consisting of

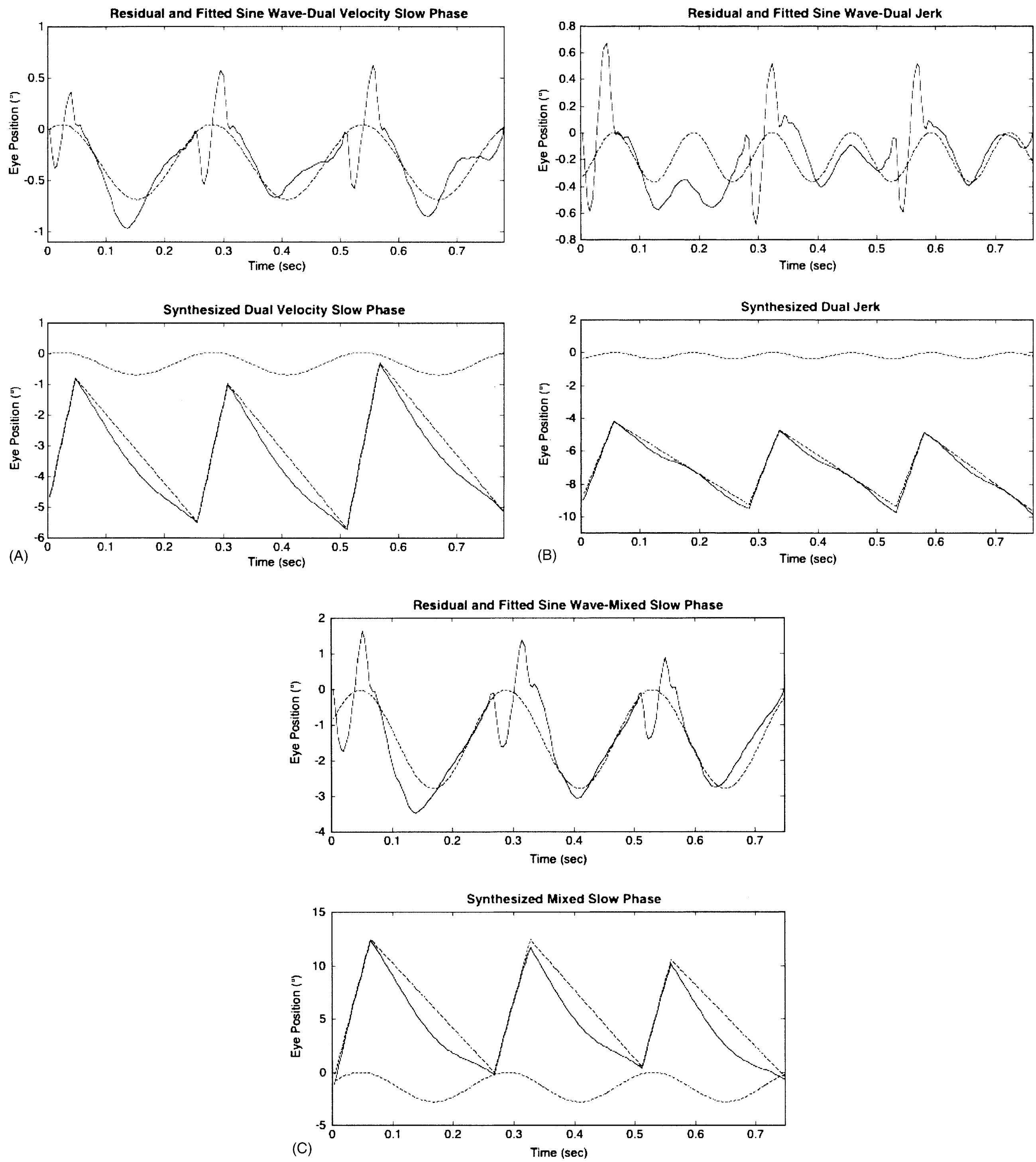

Fig. 10. (A) Dual-velocity residual (solid) and fitted sine wave (dashed). Bottom panel: Reconstruction of the dual-velocity waveform (solid) from the sinusoidal and sawtooth components (dashed). (B) Dual jerk residual (solid) and fitted sine wave (dashed). Bottom panel: Reconstruction of the dual jerk waveform (solid) from the sinusoidal and sawtooth components (dashed). (C) Mixed slow-phase residual (solid) and fitted sine wave (dashed). Bottom panel: Reconstruction of the mixed slow-phase waveform (solid) from the sinusoidal and sawtooth components (dashed).

several types of nystagmus with specific waveforms that are the result of distinct instabilities in *different* ocular motor subsystems. A recent workshop on eye movements and strabismus has reflected this understanding by renaming CN as a syndrome, the "infantile nystagmus syndrome" and LMLN as the "fusion maldevelopment syndrome" (CEMAS Working Group, 2001). We hypothesize the following different types of instability responsible for many of the waveforms exhibited by subjects with the infantile nystagmus syndrome:

vestibular tonic imbalance, causing linear slow phases; and internal smooth pursuit oscillation, causing many of the low-frequency, variable-amplitude pendular and pseudopendular waveforms. To those, we add the nucleus of the optic tract oscillation, causing the low-amplitude, high-frequency pendular oscillation that is part of dual jerk nystagmus (also seen in the binocular maldevelopment syndrome). These hypotheses require further study and modeling.

Acknowledgements

We wish to thank Anthony T. Moore, MA, FRCS who provided this patient for study.

References

Abadi, R. V., & Pascal, E. (1994). Periodic alternating nystagmus in humans with albinism. *Investigative Ophthalmology and Visual Science, 35*, 4080–4086.

Abel, L. A., Traccis, S., Troost, B. T., & Dell'Osso, L. F. (1987). Saccadic trajectories change with amplitude not time. *Neuro Ophthalmology, 7*, 309–314.

CEMAS Working Group (2001). A National Eye Institute Sponsored Workshop and Publication on The Classification of Eye Movement Abnormalities and Strabismus (CEMAS). In The National Eye Institute Publications (www.nei.nih.gov). National Institutes of Health, National Eye Institute: Bethesda, MD.

Daroff, R. B., & Dell'Osso, L. F. (1974). Periodic alternating nystagmus and the shifting null. *Canadian Journal of Otolaryngology, 3*, 367–371.

Dell'Osso, L. F., & Daroff, R. B. (1975). Congenital nystagmus waveforms and foveation strategy. *Documenta Ophthalmologica, 39*, 155–182.

Dell'Osso, L. F., Shallo-Hoffmann, J., & Moore, A. T. (2000). Congenital, periodic alternating nystagmus with unusual slow-phase waveforms [ARVO Abstract]. *Investigative Ophthalmology and Visual Science, 41*, S702.

Dell'Osso, L. F., & Jacobs, J. B. (2000). A robust, normal ocular motor system model with congenital nystagmus (CN) including braking and foveating saccades. In J. A. Sharpe (Ed.), *Neuro-ophthalmology at the beginning of the New Millennium* (pp. 107–111). Englewood: Medimond Medical Publications.

Dell'Osso, L. F., Van der Steen, J., Steinman, R. M., & Collewijn, H. (1992). Foveation dynamics in congenital nystagmus III: Vestibulo-ocular reflex. *Documenta Ophthalmologica, 79*, 51–70.

Dun, S., Shallo-Hoffmann, J., & Dell'Osso, L. F. (2001). Two time-varying components can produce anomalous slow-phase appearances in congenital nystagmus (CN) [ARVO Abstract]. *Investigative Ophthalmology and Visual Science, 42*, S165.

Hoffmann, K. P. (1983). Effects of early monocular deprivation on visual input to cat nucleus of the optic tract. *Experimental Brain Research, 51*, 236–246.

Jacobs, J. B. (2001). An ocular motor system model that simulates congenital nystagmus, including braking and foveating saccades. (Ph.D. Dissertation) Biomedical Engineering, Case Western Reserve University, Cleveland, pp. 1–357.

Jacobs, J. B., & Dell'Osso, L. F. (2000). A model of congenital nystagmus (CN) incorporating braking and foveating saccades [ARVO Abstract]. *Investigative Ophthalmology and Visual Science, 41*, S701.

Leigh, R. J., Robinson, D. A., & Zee, D. S. (1981). A hypothetical explanation for periodic alternating nystagmus: instability in the optokinetic-vestibular system. *Annals of New York Academy of Sciences, 374*, 619–635.

Schmidt, D., Dell'Osso, L. F., Abel, L. A., & Daroff, R. B. (1980). Myasthenia gravis: saccadic eye movement waveforms. *Experimental Neurology, 68*, 346–364.

Shallo-Hoffmann, J., Faldon, M., & Tusa, R. J. (1999). The incidence and waveform characteristics of periodic alternating nystagmus in congenital nystagmus. *Investigative Ophthalmology and Visual Science, 40*, 2546–2553.

Tusa, R. J., Mustari, M. J., Das, V. E., & Boothe, R. G. (2002). Animal models for visual deprivation-induced strabismus and nystagmus. In H. J. Kaminsky & R. J. Leigh (Eds.), *Neurobiology of eye movements—Annals of New York Academy of Sciences, vol. 956* (pp. 346–360). New York: NYAS.